Tellus (1999), 51B, 849–861
Printed in UK – all rights reserved

TELLUS
ISSN 0280–6495

The annual fCO_2 cycle and the air–sea CO_2 flux in the sub-Antarctic Ocean

By N. METZL[1]*, B. TILBROOK[2] and A. POISSON[1], [1]*Laboratoire de Physique et Chimie Marines, UPMC-CNRS, Case 134, 4, Place Jussieu 75252 Paris, Cedex 05, France;* [2]*Antarctic CRC and CSIRO Marine Research, PO Box 1538, Hobart, Tas 7001, Australia*

(Manuscript received 3 September 1998; in final form 12 February 1999)

ABSTRACT

The sub-Antarctic zone (SAZ) lies between the subtropical convergence (STC) and the sub-Antarctic front (SAF), and is considered one of the strongest oceanic sinks of atmospheric CO_2. The strong sink results from high winds and seasonally low sea surface fugacities of CO_2 (fCO_2), relative to atmospheric fCO_2. The region of the SAZ, and immediately south, is also subject to mode and intermediate water formation, yielding a penetration of anthropogenic CO_2 below the mixed layer. A detailed analysis of continuous measurements made during the same season and year, February–March 1993, shows a coherent pattern of fCO_2 distributions at the eastern (WOCE/SR3 at about 145°E) and western edges (WOCE/I6 at 30°E) of the Indian sector of the Southern Ocean. A strong CO_2 sink develops in the Austral summer ($\Delta fCO_2 < -50$ μatm) in both the eastern (110°–150°E) and western regions (20°–90°E). The strong CO_2 sink in summer is due to the formation of a shallow seasonal mixed-layer (about 100 m). The CO_2 drawdown in the surface water is consistent with biologically mediated drawdown of carbon over summer. In austral winter, surface fCO_2 is close to equilibrium with the atmosphere ($\Delta fCO_2 \pm 5$ μatm), and the net CO_2 exchange is small compared to summer. The near-equilibrium values in winter are associated with the formation of deep winter mixed-layers (up to 700 m). For years 1992–95, the annual CO_2 uptake for the Indian Ocean sector of the sub-Antarctic Zone (40°–50°S, 20°–150°E) is estimated to be about 0.4 GtC yr^{-1}. Extrapolating this estimate to the entire sub-Antarctic zone suggests the uptake in the circumpolar SAZ is approaching 1 GtC yr^{-1}.

1. Introduction

Large-scale oceanic air–sea carbon fluxes and estimates of anthropogenic CO_2 uptake by the oceans are mainly derived from ocean general circulation models or atmospheric diagnostic models (Siegenthaler and Sarmiento, 1993). The ocean models are generally not well validated with field observations and there are large uncertainties in the estimated fluxes. The carbon budgets derived from atmospheric diagnostic models can also be in error due to poor constraints (processes considered in the carbon balance equations) and problems in accurately representing atmospheric transport. For example, Ciais et al. (1995) showed their atmospheric model predicted an unrealistic biospheric carbon sink in high southern latitudes. The predicted sink required an ocean source at similar latitudes to compensate, even though there was little independent justification for either the ocean source or biosphere sink.

New carbon observations are being made that improve regional net air–sea CO_2 flux estimates. The observations also help define the regions where large natural deviations in fCO_2 from

* Corresponding author.
e-mail: metzl@ccr.jussieu.fr

atmospheric equilibrium values mask the anthropogenic uptake signal. Measurements made on trans-ocean sections give a good idea of surface CO_2 fugacity (fCO_2) or partial pressure (pCO_2) distributions (Keeling, 1968). The high and low values of fCO_2 often covary with sea surface nutrient concentrations, indicating a biological control on the fCO_2 distributions.

The characterisation of surface fCO_2 distributions is complicated by large seasonal changes of fCO_2 in some regions (Teal and Kanwisher, 1966; Weiss et al. 1982; Peng et al. 1987). Temporal observations have been collected in subtropical and equatorial waters (Weiss et al. 1982; Feely et al. 1987; Inoue et al. 1995; Feely et al., 1997). Data have also been obtained in high latitudes (Poisson et al. 1993; Takahashi et al., 1993; Metzl et al. 1995; Wong et al., 1995), but usually for only two or three seasons of each year. The seasonal results cover relatively large scales, and the observed trends are consistent with data collected more regularly at the subtropical BATS and HOTS stations (Keeling, 1993; Bates et al., 1996; Winn et al., 1994, 1998), at station P in the North Pacific (Wong and Chan, 1991), and during the NABE experiment (Takahashi et al., 1993). The variability in the seasonal data highlights the importance of making the regional air–sea CO_2 flux estimates from observations made throughout the year.

This paper focuses on seasonal fCO_2 variability and air–sea CO_2 fluxes for the sub-Antarctic zone (SAZ). The SAZ is a circumpolar feature that lies between the subtropical convergence (STC) and the sub-Antarctic Front (SAF). Biological activity is enhanced in the SAZ, compared to regions north of the STC (Banse, 1996). Based on data that were mostly collected during Austral Summer, the SAZ is recognized as a strong CO_2 sink (Table 1).

The quantification of the air–sea carbon exchanges in the SAZ provides an important constraint for atmospheric diagnostic models. A strong oceanic sink at latitude 30–50°S is consistent with most atmospheric models (Ciais et al., 1995; Enting et al., 1995), although atmospheric data are sparse in this region. For the Indian Ocean, the presence of a strong oceanic CO_2 sink in the subtropical and sub-Antarctic zones has been inferred to explain most of the latitudinal and longitudinal gradients in atmospheric CO_2 observed in the Southern Hemisphere (Monfray et al., 1996). Atmospheric CO_2 budgets at the global scale, typically integrate the sub-Antarctic zone with the Southern Gyres, 15°S–50°S (Tans et al., 1990; Enting et al., 1995). The inclusion of the SAZ in such a broad latitudinal band may be not appropriate if large differences exist in the seasonality of the air–sea CO_2 fluxes within the 15°S–50°S band.

As calculated previously in the southwestern Indian Ocean, the oceanic CO_2 sink is greatest during austral winter in the subtropical region (Metzl et al., 1998), whereas the CO_2 sink is greatest in the SAZ during the austral summer (January–July data; Poisson et al., 1993). South of the subtropical zone, regional averages (35°S–50°S) of observed ΔfCO_2 were found to vary from -40 µatm to -20 µatm in January and from -17 to -8 µatm in August during 1991, 1992 and 1993 (Metzl et al., 1995). In contrast to these results, recent interpolation method based on ΔpCO_2 observations and climatological oceanic circulation (advective-diffusive) monthly fields, simulates a relatively homogeneous spatio-temporal ΔpCO_2 distribution in the SAZ (ΔpCO_2 between -15 µatm and 0 µatm in February and August; see Fig. 4 in Takahashi et al., 1997). The one exception is in the Confluence region of the southwestern Atlantic ocean where low ΔpCO_2 values (below -100 µatm) are observed during austral summer months (Takahashi et al., 1993). The coupling of dynamical, thermodynamical and biological processes in the SAZ is not clearly understood and causes difficulties in reconstructing sea surface fCO_2 fields with diagnostic methods (Metzl et al., 1995), semi-prognostic models (Louanchi et al., 1996), or interpolation procedures (Takahashi et al., 1997). Global ocean carbon models generally fail in attempting to reproduce both the natural carbon distribution or anthropogenic CO_2 uptake south of 35°S (Orr et al., 1997; Sabine et al., 1999).

The work presented below is aimed at better understanding the seasonal sea surface fCO_2 variations in the SAZ and improving net air–sea carbon flux estimates. The work also provides a more comprehensive data set to constrain atmospheric inverse models and to validate global ocean carbon cycle models. We first describe the sea surface fCO_2 cycle based on observations obtained by laboratories at LPCM/France and

Table 1. *Sea surface temperature and ΔfCO_2 (or ΔpCO_2) observed in the sub-Antarctic zone*

Region	SST (°C)	ΔfCO_2 or ΔpCO_2 (μatm or ppm)	Period	Reference
Atlantic				
50°W	8–10	−100/−50	Nov. 91	Schneider and Morlang (1995)
60°W–20°E	—	−40/−20	Nov.–Mar.[a)]	Takahashi et al. (1993)
60°W–10°E	10	−15	Jun.–Sep. 86	Weiss et al.(1992)
0°	8–10	−21/−11	Oct. 83	Weiss et al. (1992)
0°	10–13	−41/−16	Jan. 84	Weiss et al. (1992)
10°E	10	−11	Mar. 90	Chipman et al. (1994)
Indian				
20–30°E	8–12	−51/+9	Feb. 87	Metzl et al. (1991)
20°E	10–12	−50/−40	Jan. 93	Robertson and Watson (1995)
40°E	10–13	−40/0	Mar. 93	Robertson and Watson (1995)
50°–60°E	10–15	−80/−40	Jan.–Apr. 91	Poisson et al. (1993)
50°–60°E	10	−30	Jul. 91	Poisson et al. (1993)
60°–70°E	10	−37	Nov. 62	Waterman (1965)
75°E	10	+2	Jul. 84	Goyet et al. (1991)
75°E	14	−38	Feb. 85	Goyet et al., (1991)
150°E	13–10	−39/−9	Dec. 83	Inoue and Sugimura (1988)
115°E	7–11	−9/+11	Jan. 84	Inoue and Sugimura (1988)
115°E	8–11	−22/+8	Jan. 69	Inoue and Sugimura (1988)
Pacific				
150°–190°E	—	−30/+10	68–72	Miyake et al. (1974)
170°E	10	−26	Feb. 61	Keeling et al. (1965)
180°	10–13	−36	Feb. 61	Keeling et al. (1965)
170–150°W	—	−20/−10	Mar. 84	Murphy et al. (1991)
100–140°W	—	0/+30	68–72	Miyake et al. (1974)
100–130°W	—	0/+10	Mar. 89	Murphy et al. (1991)
126°W	8	−25	Dec. 92	Sabine and Key (1998)
120°W	10	−4	Dec. 57	Keeling et al. (1965)

[a)] Years 84, 87, 88, 89, 90.

Where ranges are reported, the minimum and maximum values of ΔfCO_2 or ΔpCO_2 are listed. When only sea water pCO_2 is given, calculation of ΔfCO_2 (fCO_{2ocean}–fCO_{2air}, or ΔpCO_2, in μatm or ppm, depending of the original information) has been made according to the atmospheric concentration for the corresponding period and year based on $\times CO_2$ (in ppm) measurements at South Pole (Keeling and Whorf, 1996) and at 100% water vapor saturation at SST = 10°C, Salinity = 34, using the equations given by Weiss and Price (1980).

CSIRO/Australia (Fig. 1). An annual cycle of fCO_2 is then extracted by combining the two data sets, and a net air–sea CO_2 flux is estimated for the SAZ.

2. The monthly sea surface fCO_2 cycle in the SAZ

2.1. Data collections for the sub-Antarctic region

The fCO_2 measurements techniques have been described in detail by Poisson et al. (1993) for LPCM data (MINERVE cruises onboard the *RSV Marion-Dufresne*). The CSIRO data were obtained on repeat cruises made on the *RSV Aurora Australis* and were collected using a system similar to the continuous system described in Wanninkhof and Thoning (1993). Both laboratories continuously monitor surface fCO_2 using automated infrared spectrometric techniques (Siemens for LPCM and LICOR for CSIRO). The systems measure CO_2 in a closed loop of air that has been continuously equilibrated with surface seawater (intake depths below sea level are 5 m for LPCM and 7 m for CSIRO). The equilibrium cells are thermostated with surface seawater and the temperature in the cells is usually less than 1°C

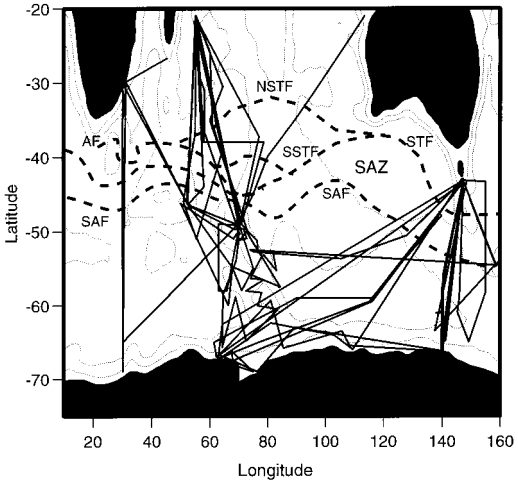

Fig. 1. Tracks of the LPCM and CSIRO cruises in the South Indian Ocean. In this study, we analyse the sea surface fCO_2 data obtained in the sub-Antarctic zone (SAZ) that lies between the subtropical fronts (STF) and the sub-Antarctic Front (SAF). In the south Indian Ocean, the frontal structure is composed by the Aghulas Front (AF), the North Subtropical Front (NSTF) and the South Subtropical Front (SSTF). Fronts positions adapted from Belkin and Gordon (1996).

warmer than the sea surface temperature (SST). Calibrations against CO_2-in-air standard gases are made every 7 h for LPCM and each 3 h for CSIRO. The LPCM system records 10 min averages of continuous measurements, and CSIRO records averages every 4 min. To convert measurements to in situ fCO_2 data, saturated vapor pressure is calculated using Weiss and Price (1980) polynomials. A correction to in situ temperature is made using the formulae of Copin-Montégut (1988, 1989). The two laboratories have participated in an international intercalibration exercise in June 1996 onboard R.V. Meteor. The LPCM and CSIRO data compare well, with deviations between both data sets smaller than ± 2 µatm over a broad range of fCO_2 values (Koertzinger et al., 1998). The difference of ± 2 µatm lies within the range of measurements precisions of about ± 1 µatm estimated for LPCM and ± 0.7 µatm estimated for CSIRO.

2.2. *Sea surface fCO_2 distributions*

There is a coherent meridional pattern of fCO_2 variations for measurements made during the same season and year (February–March 1993), at the eastern (WOCE/SR3 at about 145°E) and western (WOCE/I6-CIVA at 30°E) edges of the Indian sector of the Southern Ocean (Fig. 2). Low fCO_2 values are observed near pack-ice south of the Antarctic Divergence, and are related to biological activity in summer (Metzl et al., 1991; Poisson et al., 1994). Further north, fCO_2 minima also occur at about the same temperature (14°C), and are localized in the SAZ at 42°S in the west and 45°S in the east. Such low fCO_2 values during summer have been observed in all sub-Antarctic regions of the oceans (Table 1).

The data listed in Table 1 show that the SAZ is typically undersaturated ($\Delta fCO_2 < 0$), except for some periods in the eastern Pacific. The meridional distributions shown in Fig. 2 and described in some of the cruises listed in Table 1 indicate that a strong fCO_2 gradient is typical across the SAZ. The highest fCO_2 values generally occur towards

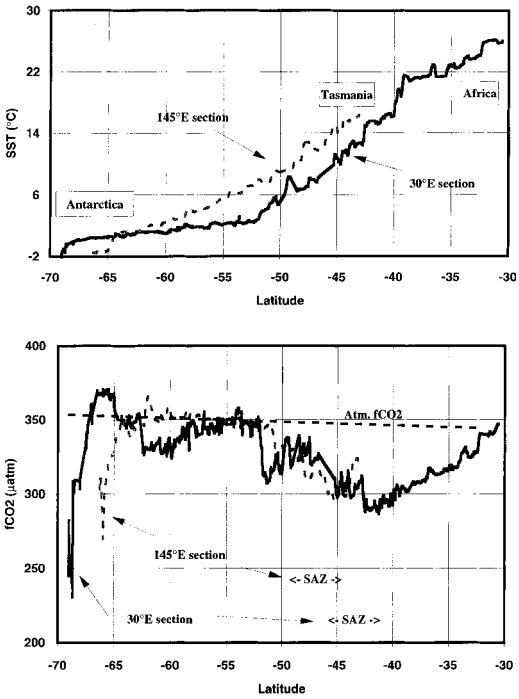

Fig. 2. Sea surface temperature (°C) and fCO_2 (µatm) observed in February–March 1993 along 30°E (Africa to Antarctica, black line) and along 145°E (Tasmania to Antarctica, dashed-grey line). The lowest fCO_2 are observed in the SAZ on both sections and in the seasonal sea–ice zone south of 65°S.

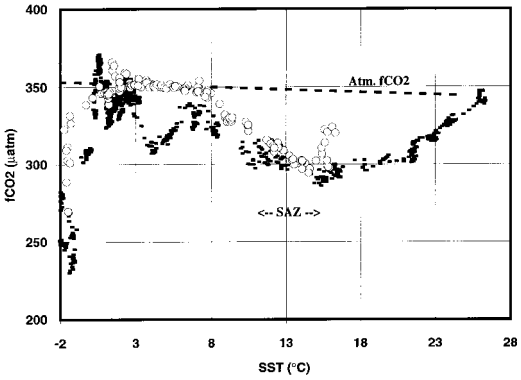

Fig. 3. fCO_2/SST relationship for data presented in Fig. 2. The track at 30°E is represented by black squares, the track around 145°E by open circles.

the SAF (the southern boundary of the SAZ). Thus, higher fCO_2 in the SAZ occurs at lower SST (Fig. 3). The central and eastern sub-Antarctic Indian Ocean data (Fig. 4) also show sea surface fCO_2 is higher in austral winter (August, 1993) than summer (February–March 1993). The fCO_2 minima located in the SAZ in summer are not observed in winter. Based on our measurements and a few other SAZ observations made between July and September in Table 1, it appears that fCO_2 is higher in winter than summer (the absolute value of ΔfCO_2 is smaller).

2.3. *Averaged sea surface fCO_2 cycle in the SAZ*

In order to extract the monthly sea surface CO_2 cycle, we averaged the continuous measurements for each cruise and month, at a scale of $1° \times 1°$ (the scale that can be reached by Global Ocean Carbon Cycle Models). The monthly cycles observed in the central (41°S/55–75°E) and eastern (45°S/135–155°E) regions of the Indian Ocean SAZ show a clear seasonal signal (Fig. 5a). The seasonal amplitude is about 50 µatm in both regions, which is comparable to the seasonal amplitude observed in subtropical waters (Winn et al., 1994; Bates et al., 1996; Metzl et al., 1998), but there is about a 6 months phase shift in the signal compared to the subtropics.

The seasonal fCO_2 cycle in the SAZ cannot be explained by SST variations. The low fCO_2 occurs in austral summer (December to February) and high values occur during late winter (August to

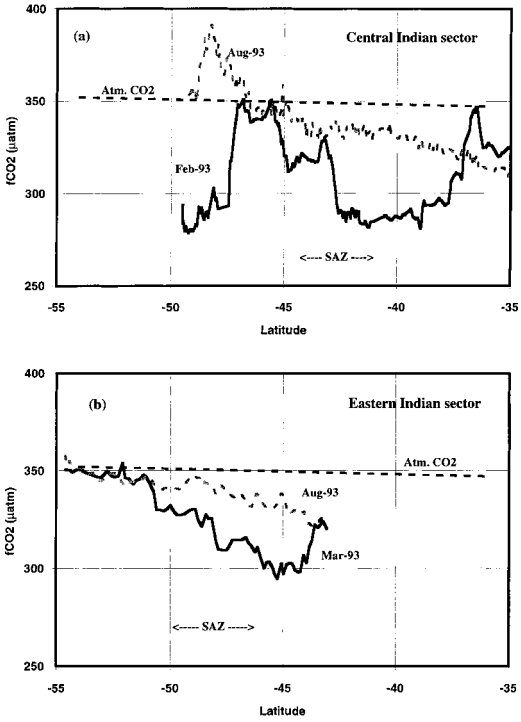

Fig. 4. Sea surface fCO_2 observed along the same tracks in summer (black line) and winter (dashed-grey line) in the central Indian Ocean (a) and the eastern Indian Ocean (b). The fCO_2 values are highest in winter for both SAZ regions.

September). Consequently, the "meridional" fCO_2/SST relationship extracted from single cruise data (Fig. 3) and the "temporal" fCO_2/SST relationship are both negative (Fig. 5b). This relationship is opposite that observed in the subtropics (Metzl et al., 1998) and opposite the temperature effect on fCO_2. Low fCO_2 in summer could be related to biological activity dominating the effect of warming. This process appears to be most pronounced in the central Indian basin during February where fCO_2 values as low as 280 µatm are observed each year (Fig. 5). The low values in the central Indian sector in February appear to be related to the confluence of multiple hydrological fronts (Fig. 1) including the Agulhas Front (AF), the STC, and the SAF (Belkin and Gordon, 1996). High fCO_2 values in winter are likely to

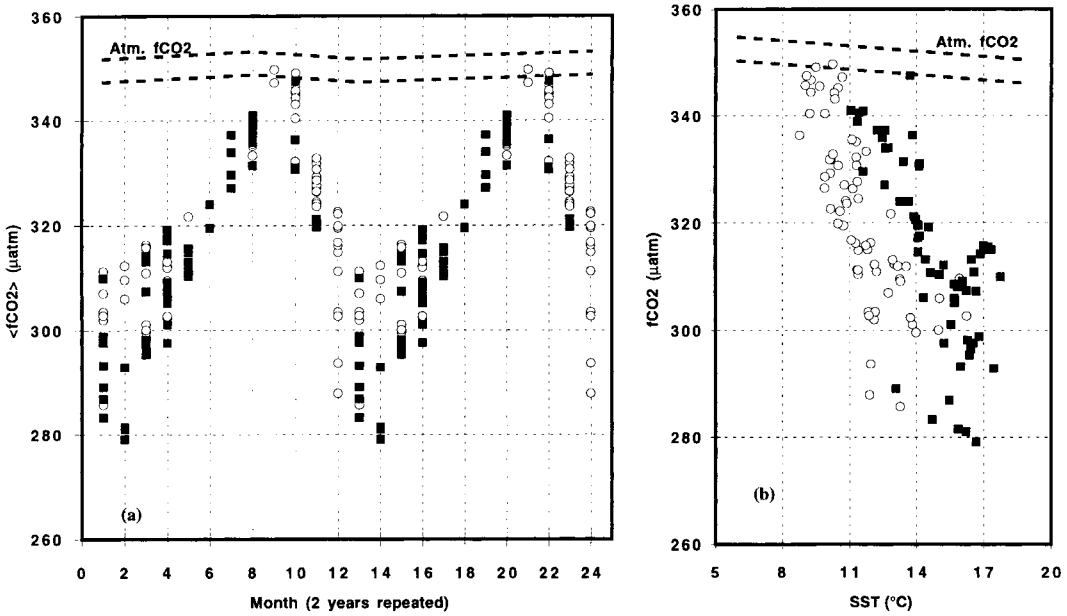

Fig. 5. (a) The annual cycle of fCO_2 observed in the SAZ of the Indian Ocean deduced from mean monthly observations ($1° \times 1°$) for the central region (black squares) and eastern sector (open circles). The seasonal pattern is repeated to highlight the annual cycle. The dashed lines indicates average atmospheric fCO_2 for years 1992 and 1995; (b) the relationship fCO_2/SST for the same regions (same symbols).

be related to strong mixing with CO_2-rich subsurface waters. Winter mixed layers as deep as 700 m have been observed in the eastern SAZ (Rintoul et al., 1997). In the central region of the Indian Ocean, we recently recorded deep mixed layers in the SAZ (520 m at 40°S) during austral winter (cruise OISO-2, August–September 1998, onboard *RSV Marion-Dufresne*).

2.4. *Seasonal variation of the carbon system (TA, DIC) in the SAZ*

The salinity presents almost no seasonal signal in the SAZ (Rintoul et al. 1997). It is the same for Total Alkalinity (TA). Using data obtained in the central and the eastern region of the Indian Ocean during different seasons (INDIGO-1 in April 1985, INDIGO-3 in February 1987, and WOCE/SR3 in August 1996), we found a close agreement between the different TA/SSS regressions (Fig. 6). This shows the distribution of TA in the SAZ can be predicted from salinity, and suggests that the seasonal variations of total dissolved inorganic carbon (DIC) reflects mostly the fCO_2 cycle, the latter being opposite to SST.

The annual cycle of DIC can be calculated from monthly averaged of fCO_2, TA, SST and SSS, (Fig. 7). The DIC concentrations vary from 2006 µmol kg^{-1} in February (corresponding to the low fCO_2 observed in the central region) to 2080 µmol kg^{-1} in August. The average summer value (January–March) of 2025 µmol kg^{-1} is 50 µmol kg^{-1} lower than the average winter time value (June–August).

The above estimate of the seasonal amplitude of the DIC cycle in the SAZ is consistent with observations from Goyet et al. (1991). They observed higher DIC in July 1984 compared to late March 1985, for the central Indian Ocean. The largest difference of 30 µmol kg^{-1} reported by Goyet et al. (1991) occurred in the SAZ, and is similar to the range of variations we estimate from our calculation (about 40 µmol kg^{-1} from March–April to July, Fig. 7). The DIC concentration measured in late March 1985 by Goyet et al. (1991) was about 2040 µmol kg^{-1} (or 2030 µmol kg^{-1} after applying the corrections proposed by Sabine et al. (1999) for INDIGO-1 data), which is similar to our estimate DIC value for

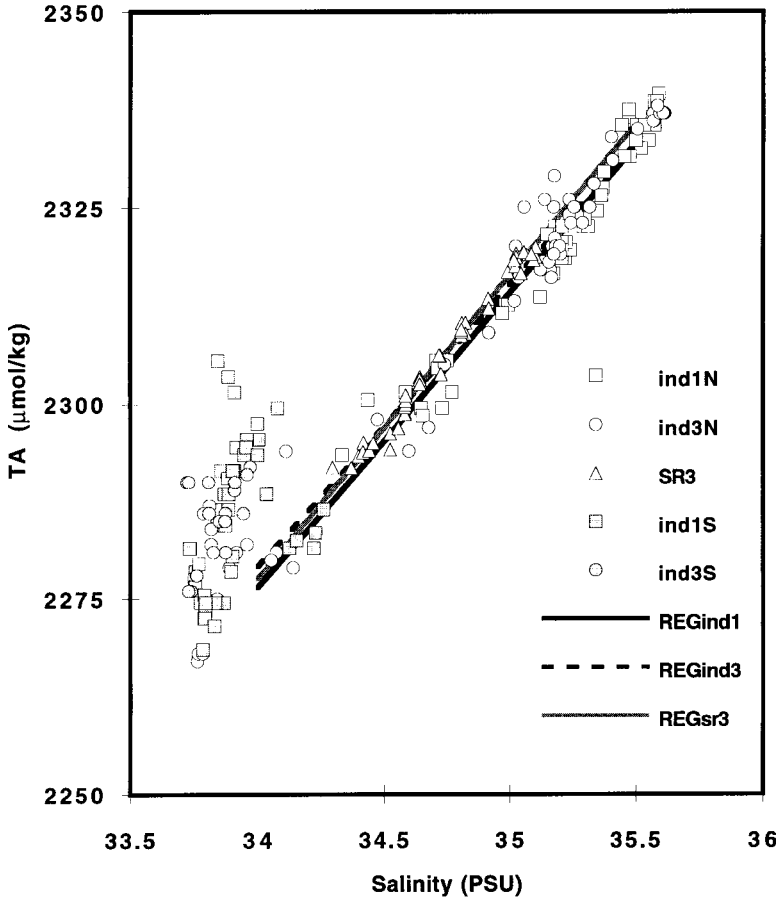

Fig. 6. The TA/SSS relationship observed in the South-West Indian Ocean during INDIGO-1 (March–April 1985) and INDIGO-3 cruises (January–February 1987), and in the South-East Indian Ocean during the WOCE/SR3 cruise (August 1996). Based on a recent comparison study between INDIGO and US/WOCE stations (Sabine et al., 1999) we have corrected the INDIGO-1 TA values by -6.5 µmol kg^{-1}. The TA/SSS relation is different north (open symbols) and south (filled symbols) of the SAF. The line, dashed line and grey line represents the linear regressions calculated for the three cruises from the observations north of the SAF: $TA = 998.74 + 37.580 \cdot S$ ($r^2 = 0.952$, $n = 57$) for IND-1; $TA = 1055.9 + 35.978 \cdot S$ ($r^2 = 0.972$, $n = 61$) for IND-3; $TA = 960.5 + 38.736 \cdot S$ ($r^2 = 0.983$, $n = 108$) for WOCE/SR3.

March–April. The seasonal amplitude of DIC calculated for the SAZ is about the same as in the North Atlantic (47°N, Takahashi et al, 1993), and smaller than the 100 µmol kg^{-1} variations observed in the subarctic region of the Pacific (Takahashi et al., 1993). The calculated amplitude is larger than observations from the subtropical North Atlantic (30 to 40 µmol kg^{-1}; Keeling, 1993, Bates et al., 1996), at the JGOFS/KERFIX time series station in the Polar Frontal zone of the Southern Ocean (about 20 µmol kg^{-1}; Jeandel et al., 1998), and in the Weddell Sea (less than 15 µmol kg^{-1} based on a comparison of summer and winter data; Hoppema et al., 1995).

The decrease in fCO_2 from October to February coincides with DIC and nutrient concentration decreases, and could result from increased biological uptake of CO_2. There are indications of higher Chl-a concentrations during December–January in the SAZ of the Indian Ocean (Banse, 1996). However, this region shows a relatively small seasonal change in chlorophyll concentra-

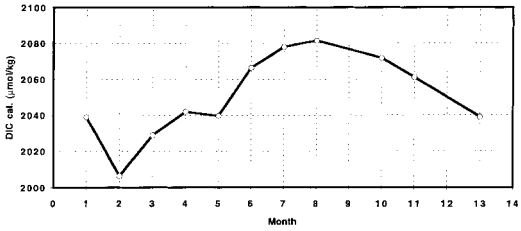

Fig. 7. Annual cycle of sea surface DIC (μmol kg^{-1}) in the SAZ of Central Indian Ocean. Each point represents the monthly average obtained in the region 40–41°S/55–75°E. The DIC cycle was computed from the monthly values of sea surface fCO_2, TA, SST and SSS. We used the CO_2sys program version 1.04 provided by Lewis and Wallace (1998) for the calculation, with the dissociations constants of Goyet and Poisson (1989). Note that the average DIC cycle calculated in this way would differ only by about 0.5 μmol kg^{-1} when using individual values of fCO_2 (Fig. 5a) and then averaging the calculated DIC for each month to produce Fig. 7.

tions when the data are averaged (e.g., CZCS climatology). If the observed DIC decrease was entirely due to net biological carbon drawdown, the calculated spring–summer diminution of DIC would correspond to a Net Community Production of 4 to 13 mgC m^{-3} d^{-1}, depending on the month. When integrated over 50 m, this range of net production corresponds to 0.2 to 0.6 gC m^{-2} d^{-1} or 80 to 240 gC m^{-2} yr^{-1}. The highest value of 13 mgC m^{-3} d^{-1} is calculated in February when DIC is minimum. This is about half the primary production of 22.5 mgC m^{-3} d^{-1} reported by Jacques and Minas (1981) for measurements made in late March 1977 at 43°S in the Central Indian Ocean.

In winter the calculated DIC concentration is about 2080 μmol kg^{-1}. Assuming biology has little effect on CO_2 variation during winter (the photosynthesic decrease of CO_2 is equal to the increase due to remineralization), the calculated air–sea CO_2 fluxes would cause an increase of about 8 μmol kg^{-1} over 180 days (based on fluxes estimated in the next section). The surface layer in summer has to be mixed with water as deep as 300–400 m in order to produce DIC concentrations higher than 2080 μmol kg^{-1} (the concentrations observed in the SAZ below 200 m). The near-equilibrium fCO_2 values observed in late winter are clearly linked to the formation of deep winter mixed-layers in the SAZ. In order to get realistic seasonal DIC variations and therefore realistic air–sea CO_2 fluxes at large scale, it is desirable that global ocean models reproduce winter deep mixed-layers in this region.

3. Air–sea CO_2 fluxes in the SAZ

The annual fCO_2 cycles obtained in the central and eastern Indian Ocean (Fig. 5) were similar. If we assume the two regions are representative of the entire circumpolar SAZ, our results can be used to compute an integrated flux over the SAZ. The flux is determined by the expression $F = K \cdot \Delta fCO_2$, where ΔfCO_2 is the difference between sea surface fCO_2 and atmospheric fCO_2, and K is the gas transfer coefficient (the product of the piston velocity and solubility). The monthly means fluxes (Fig. 8) are obtained by averaging for each month the individual fluxes calculated for each $1^\circ \times 1^\circ$ pixel in the SAZ. For sensitivity analysis different atmospheric CO_2 concentrations will be used (1992, 1995 or the average for the period 1992 to 1995). In air–sea gas flux calcula-

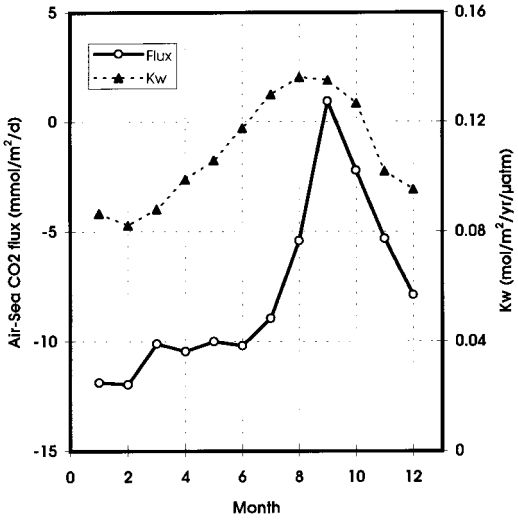

Fig. 8. Monthly mean of the gas transfer coefficient (closed triangles) and air–sea CO_2 fluxes (open circles) in the Indian Ocean SAZ. A negative air–sea CO_2 flux represents an oceanic CO_2 sink. The values of K_W estimated by Boutin and Etcheto (1997) for each 2.5° latitudinal band in the Indian Ocean have been averaged from 40°S to 52°S. The large sink during austral summer is observed when K_W is lower. The annual cycle of the air–sea CO_2 flux in the SAZ is mainly controlled by sea surface fCO_2 variability (Fig. 5).

tions, a large error is associated to the value of K depending on the piston velocity (k) versus wind speed relation, especially when the winds are high, as they are in the SAZ. For the summer and winter cruises in the Indian Ocean SAZ, the average winds speed was 10.2 m s^{-1} ($\pm$2.4). Based on these ship winds, we have compared the values of k calculated with the formulae of Wanninkhof (1992), k_W, with those determined using the equations of Liss and Merlivat (1986), k_{LM}. In the SAZ, the average k_W, is 0.11 ($\pm$0.04) cm h^{-1} compared 0.06 ($\pm$0.02) cm h^{-1} for k_{LM}. The ratio k_W/k_{LM} is 1.88. In a recent experiment of dual tracer (SF_6, ^3He) in a large fresh water lake of the Kerguelen Archipelago (49°S, in the Indian Ocean) where winds ranged between 1 and 10 m s^{-1}, Jean-Baptiste and Poisson (1999) obtained gas transfer velocities values consistent with high CO_2 transfer velocity like those derived from ^{14}C oceanic inventories or open ocean experiments. To calculate k in the SAZ, we thus select the relation proposed by Wanninkhof (1992), which lies within the results of these fields studies. To compare our results with previous air–sea CO_2 fluxes estimated with the k-wind speed relation proposed by Liss and Merlivat (1986) instead of Wanninkhof (1992), the fluxes presented below must be divided by 1.9.

To calculate monthly air–sea CO_2 fluxes integrated in the Indian Ocean SAZ we use the monthly mean values of the gas transfer coefficient, K_W, as estimated by Boutin and Etcheto (1997) using SSMI-derived wind fields for the years 1988–92 and between 22°30′E to 147°30′E. Fig. 8 shows that K_W varies seasonally in the SAZ with relatively low values in February (0.08 mol m^{-2} yr^{-1} µatm^{-1}) and high values in August–September (0.14 mol m^{-2} yr^{-1} µatm^{-1}). The yearly mean of K_W from SSMI is 0.11 ($\pm$0.02) mol m^{-2} yr^{-1} µatm^{-1}. The same calculation using the winds measured during cruises in the south-western Indian Ocean results in an annual value of K_W of 0.10 mol m^{-2} yr^{-1} µatm^{-1}, which is close to the mean annual value of K_W derived from SSMI winds.

The calculated monthly air–sea CO_2 fluxes are also shown in Fig. 8. The flux varies between -12 mmol m^{-2} d^{-1} in summer (a CO_2 sink) to less than $+1$ mmol m^{-2} d^{-1} in winter (a small CO_2 source). The sum of the monthly fluxes leads to an annual sink of -2.84 mol m^{-2} yr^{-1}. A value of -3.00 mol m^{-2} yr^{-1} that would result from using a constant K_W of 0.10 mol m^{-2} yr^{-1} µatm^{-1} for each month. Thus, the seasonal air–sea CO_2 flux in the SAZ is mainly controlled by the seasonal variations of sea surface fCO_2, and temporal changes in the value of K_W are secondary in determining the magnitude of the net air–sea flux for this region. If we use the monthly mean oceanic fCO_2 data shown in Fig. 5 and atmospheric CO_2 concentration of 353.5 ppm (year 1992), the annual sink is -2.73 mol m^{-2} yr^{-1}. The same calculation with atmospheric CO_2 concentration of 358 ppm (year 1995) leads to an annual sink of -3.22 mol m^{-2} yr^{-1}. A value of -2.95 mol m^{-2} yr^{-1} is obtained when using the average atmospheric concentration of 356 ppm for the years 1992–1995.

For the Indian Ocean SAZ, taken here between 40°S and 50°S, the annual oceanic carbon sink is 0.38 GtC yr^{-1} for the period 1992–95. Values of 0.36 GtC yr^{-1} and 0.42 GtC yr^{-1} are obtained for the years 1992 and 1995 respectively. Assuming that the fCO_2 cycles obtained in the western and eastern Indian Ocean SAZ are representative of the entire SAZ, and the same for atmospheric fCO_2 and wind fields, an extrapolation of the monthly fluxes to the entire SAZ (40°S–50°S band) leads to an estimated annual CO_2 uptake of 1.05 GtC yr^{-1} (period 1992–95). However, during austral winter, winds (and therefore K_W) are higher in the Indian Ocean compared to Atlantic and Pacific (Boutin and Etcheto, 1997). For example, during August, K_W values in the SAZ are about 30% less in the Pacific compared to the Indian sector. Taking into account the regional distribution of K_W and areas of the SAZ in each basin, we obtained an annual CO_2 sink of 0.24 GtC yr^{-1} and 0.31 GtC yr^{-1} for the SAZ Atlantic and Pacific sectors respectively. The sum of the three sectors leads to a circumpolar SAZ CO_2 sink of 0.93 GtC yr^{-1} which is 11% smaller than the direct extrapolation derived from Indian fluxes alone (1.05 GtC yr^{-1}). For this estimation we assumed the ΔfCO_2 cycle obtained in the Indian sector is the same in other regions.

The ΔfCO_2 compilation presented on Table 1 indicates that in the southwestern Atlantic, very low ΔfCO_2 (-100 µatm) have been observed in summer (Takahashi et al., 1993) and average ΔfCO_2 during winter (June–September) is about -15 µatm (Weiss et al., 1992). For the Pacific sector, ΔfCO_2 data have been obtained mainly

during austral summer (December–February). Observations in March (Murphy et al., 1991) indicates an oceanic CO_2 sink with ΔfCO_2 between -20 to -10 μatm in the central Pacific, with a small source, not higher than 10 μatm in the eastern Pacific. These data suggests the extrapolation based on the sea surface fCO_2 cycle in the Indian Ocean could underestimate the sink in the Atlantic SAZ and overestimate the sink in the Pacific SAZ. New data during winter in the Pacific and a more complete compilation of fCO_2 observations will help to better estimate the air–sea CO_2 fluxes in the entire SAZ, which could represent a large CO_2 sink approaching 1 GtC yr^{-1}.

4. Concluding remarks

The SAZ can be viewed as a region of carbon export through biological processes and the export of anthropogenic CO_2 through dynamical processes such as the formation of mode waters. The data presented, cover a series of cruises in the Indian Ocean for the period 1991–1995, and show a coherent annual cycle in sea-surface carbon dioxide concentrations. The seasonal amplitude in fCO_2 in the SAZ of about 50 μatm, is as large as in the subtropics, but has the opposite phase with a fCO_2 minimum in austral summer and a maximum in winter. The fCO_2 cycle in the SAZ opposes the temperature effect on fCO_2. The processes that explain the seasonal evolution are clearly related to biological activity in summer and deep mixing in winter. These processes have to be taken into account and reproduced in global carbon cycle models to simulate realistic seasonal amplitude of both fCO_2 and DIC.

Apart from late winter, the SAZ was a sink for CO_2 in both the central and eastern Indian Ocean. For the region, the CO_2 sink was about 0.38 GtC yr^{-1} (period 1992–95) which is similar in magnitude to the CO_2 source estimated to be between 0.3 to 0.7 GtC yr^{-1} for the equatorial Pacific during the years 1992–1994 (Feely et al. 1997). This comparison based on the same years of observations (nineties) and the same gas transfer coefficient formulation (Wanninkhof, 1992), emphasizes the importance of the SAZ in the carbon cycle. Assuming that the fCO_2 cycles obtained in the western and eastern Indian Ocean SAZ are representative for the entire SAZ, a zonal extrapolation of the fluxes obtained in the Indian SAZ to the entire SAZ leads to an estimated annual CO_2 uptake of about 1 GtC yr^{-1}. This sink based on oceanic data is much larger compared to air–sea fluxes estimates based on atmospheric data (Ciais et al., 1995). For the region 35°S–45°S the 2D atmospheric model of Ciais et al. calculates an oceanic CO_2 sink of 0.14 GtC yr^{-1} in 1992 and 0.37 GtC yr^{-1} in 1993. For the zone 45°S–55°S the 2D model calculates a CO_2 source of 0.11 GtC yr^{-1} in 1992, and 0.38 GtC yr^{-1} in 1993. Although large scale climatic events such as ENSO are not documented in the SAZ, future investigations of interannual variability of the air–sea fluxes in the SAZ are needed to estimate the range of natural variability (as it has been compiled for the Equatorial Pacific; Feely et al., 1997), and to compare directly with interannual estimates derived from atmospheric inverse methods.

The climatological fCO_2 cycle constructed in this study will provide a useful set of data to constraint atmospheric inverse models that attempt to quantify regional and interannual variability of terrestrial and ocean sources and sinks of carbon. The data set can also be used for validating global ocean carbon cycle models. At present, global ocean models are not reproducing mixed layers as deep as those observed in winter in the SAZ and there are difficulties in modelling realistic seasonal primary production in temperate and high latitudes of the southern ocean. A more thorough understanding of the processes controlling the CO_2 cycle in the SAZ will require more complete descriptions of the temporal variations (seasonal and interannual if possible) of biogeochemical properties in both surface and subsurface waters.

5. Acknowledgments

This study was initiated through support from the French–Australia cooperation program (INSU/CNRS) and the Australian Department of Industry, Science and Technology. We thank C. Le Provost, coordinator of this cooperation program. The MINERVE observational program onboard the *RSV Marion-Dufresne* was sponsored by Institut Français pour la Recherche et la Technologie Polaires (IFRTP) and was also sup-

ported by the French program PNEDC/CO_2 and the European programs EPOCH and ESCOBA. We thank Y. Balut for his assistance in the organisation of the MINERVE program and B. Ollivier for his continuous help during cruises. We also thank all the captains and crews of the *RSV Marion-Dufresne* and the *RSV Aurora Australis*. The Australian component of the work was supported in part by Environment Australia through the CSIRO Climate Change Research Program. H. Beggs is acknowledged for running the fCO_2 equipment on some voyages of *RSV Aurora Australis*, and M. Pretty for helping maintain the equipment. R. Matear and T. Trull provided useful comments on the initial manuscript. S. Rintoul helped with discussions on the seasonal variability of water masses and mixed layer depths in the regions studied.

REFERENCES

Banse, K. 1996. Low seasonality of low concentrations of surface chlorophyll in the sub-Antarctic water ring: underwater irradiance, iron, or grazing? *Prog. Ocean.* **37**, 241–291.

Bates, N. R., Michaels, A. F. and Knap, A. H. 1996. Seasonal and interannual variability of the oceanic carbon dioxide species at the US JGOFS Bermuda Atlantic Times-series Study (BATS) site. *Deep-Sea Res.* **43**, 347–383.

Belkin, I. and Gordon, A. 1996. Southern Ocean fronts from the Greenwich meridian to Tasmania. *J. Geophys. Res.* **101**, C2, 3675–3696.

Boutin, J. and Etcheto, J. 1997. Long-term variability of the air–sea CO_2 exchange coefficient: Consequences for the CO_2 fluxes in the Equatorial Pacific Ocean. *Global Biogeochem. Cycle* **11**, 453–470.

Ciais, P., Tans, P. P., White, J. W. C., Trolier, M. and Francey, R. 1995. A large northern hemisphere terrestrial CO_2 sink indicated by the 13C/12C ratio of atmospheric CO_2. *Science* **269**, 1098–1102.

Chipman, D. W., Takahashi, T., Breger, D. and Sutherland, S. C. 1994. *Carbon dioxide, hydrographic and chemical data obtained during the R/V Meteor cruise 11/5 in the South Atlantic and northern Weddell sea areas* (WOCE sections A-12 and A-21). ORNL/CDIAC-55, NDP-045. Carbon Dioxide Information Analysis Center, Oak Ridge National Laboratory, US Department of Energy, Oak Ridge, Tennessee, USA, 56 pp.

Copin-Montégut, C. 1988. A new formula for the effect of temperature on the partial pressure of CO_2 in seawater. *Mar. Chem.* **25**, 29–37.

Copin-Montégut, C. 1989. A new formula for the effect of temperature on the partial pressure of CO_2 in seawater. Corrigendum. *Mar. Chem.* **27**, 143–144.

Enting, I., Trudinger, C. and Francey, R. 1995. A synthesis inversion of the concentration and $\delta^{13}C$ of atmospheric CO_2. *Tellus* **47B**, 35–52.

Feely, R. A., Gammon, R. H., Taft, B. A., Pullen, P. E., Waterman, L. S., Conway, T. J., Gendron, J. F. and Wisegarver, D. P. 1987. Distribution of chemical tracers in the eastern equatorial Pacific during and after the 1982–83 El Niño/Southern Oscillation Event. *J. Geophys. Res.* **92**, C6, 6545–6558.

Feely, R. A., Wanninkhof, R., Goyet, C., Archer, D. E. and Takahashi, T. 1997. Variability of CO_2 distributions and sea–air fluxes in the central equatorial Pacific during the 1991–94 El Niño. *Deep-Sea Res.* **44**, 9–10, 1851–1868.

Goyet, C. and Poisson, A. 1989. New determination of carbonic acid dissociation constants in seawater as a function of temperature and salinity. *Deep-Sea Res.* **36**, 11, 1635–1654.

Goyet, C., Beauverger, C., Brunet, C. and Poisson, A. 1991. Distribution of carbon dioxide partial pressure in surface waters of the southwest Indian Ocean. *Tellus* **43B**, 1–11.

Hoppema, M., Fahrbach, E., Schröder, M., Wisotzki, A., de Baar, H. 1995. Winter–summer differences of carbon dioxide and oxygen in the Weddell Sea surface layer. *Mar. Chem.* **51**, 177–192.

Inoue, H. Y. and Sugimura, Y. 1988. Distribution and variations of oceanic carbon dioxide in the western North Pacific, eastern Indian and Southern Ocean south of Australia. *Tellus* **40B**, 308–320.

Inoue, H. Y., Matsueda, H., Ishii, H., Fushimi, K., Hirota, M., Asanuma, I. and Takasugi, Y. 1995. Long-term trend of the partial pressure of carbon dioxide (pCO_2) in surface waters of the western North Pacific, 1984–1993. *Tellus* **47B**, 391–413.

Jacques, G. and Minas, M. 1981. Production primare dans le secteur indien de l'Océan Antarctique en fin d'été, *Oceanologica Acta* **4**, 33–41.

Jean-Baptiste, P. and Poisson, A. 1999. Gas transer experiment on a lake (Kerguelen Islands) using ^3He and SF_6. *J. Geophys. Res.*, in press.

Jeandel, C., Ruiz-Pino, D., Gjata, E., Poisson, A., Brunet, C., Charriaud, E. Dehairs, F., Delille, D., Fiala, M., Fravalo, C., Miquel, J. C., Park, Y.-H., Razouls, S., Quéguiner, B., Schauer, B. and Tréguer, P. 1998. KERFIX, a permanent time series station in the Southern ocean: a presentation. *J. Marine Systems* **17**, 1–4, 555–569.

Keeling, C. D. 1968. Carbon dioxide in surface ocean waters 4. Global distribution. *J. Geophys. Res.* **73**, 14, 4543–4553.

Keeling, C. D. 1993. Surface ocean CO_2. In: *The global carbon cycle,* NATO ASI Series, Vol. I, 15 (ed. Heimman, M.). Springer-Verlag, Berlin Heidelberg, 413–429.

Keeling, C. D., Rakestaw, N. W. and Waterman, L. S. 1965. Carbon dioxide in surface waters of the Pacific Ocean 1. Measurements of the distribution. *J. Geophys. Res.* **70**, 24, 6087–6097.

Keeling, C. D. and Whorf, T. P. 1996. Atmospheric CO_2 records from sites in the SIO air sampling network. In: *Trends: a compendium of data on global change*. Carbon Dioxide Information Analysis Center, Oak Ridge National Laboratory, Oak Ridge, Tennessee, USA.

Koertzinger, A., Mintrop, L. and Duinker, J. C. 1998. *The international intercomparison exercise of underway fCO_2 systems during the R/V Meteor Cruise 36/1 in the North Atlantic Ocean.* CDIAC-NDP067. Carbon Dioxide Information Analysis Center, Oak Ridge National Laboratory, Oak Ridge, Tennessee, USA.

Lewis, E. and Wallace, D. W. R. 1998. *Program developed for CO_2 system calculations.* ORNL/CDIAC-105. Carbon Dioxide Information Analysis Center, Oak Ridge National Laboratory, US Department of Energy, Oak Ridge, Tennessee, USA.

Liss, P. and Merlivat, L. 1986. Air–sea exchange rates, introduction and synthesis. In: *The rôle of air–sea exchange in geochemical cycling* (ed. Buat-Ménard, P.). NATO/ASI Series, D. Reidel, Dordrecht, 113–127.

Louanchi, F., Metzl, N. and Poisson, A. 1996. Modelling the monthly sea surface fCO_2 fields in the Indian Ocean. *Marine Chem.* **55**, 265–279.

Metzl, N., Beauverger, C., Brunet, C., Goyet, C. and Poisson, A. 1991. Surface water pCO_2 in the Western Indian Sector of the Southern Ocean: a highly variable CO_2 source/sink region during the austral summer. *Marine Chem.* **35**, 85–95.

Metzl, N., Poisson, A., Louanchi, F., Brunet, C., Schauer, B. and Brès, B. 1995. Spatio-temporal distributions of air–sea fluxes of CO_2 in the Indian and Antarctic oceans, a first step. *Tellus* **47B**, 56–69.

Metzl, N., Louanchi, F. and Poisson, A. 1998. Seasonal and interannual variations of sea surface carbon dioxide in the subtropical Indian Ocean. *Marine Chem.* **60**, 131–146.

Miyake, Y., Sugimura, Y. and Saruhashi, K. 1974. *The carbon dioxide content in the surface waters in the Pacific Ocean.* Rec. of Ocean. Works in Japan, 12, no. 2, 45–52.

Monfray, P., Ramonet, M. and Beardsmore, D. 1996. Longitudinal and vertical gradient over the subtropical/sub-Antarctic oceanic CO_2 sink. *Tellus* **48B**, 445–456.

Murphy, P., Feely, R. A., Gammon, R. H., Kelly, K. C. and Waterman, L. S. 1991. Autumn air–sea disequilibrium of CO_2 in the South Pacific Ocean. *Marine Chem.* **35**, 77–84.

Orr, J. C., Monfray, P., Sarmiento, J. L., Maier-Reimer, E., Palmer, J. R. and Najjar, R. G. 1997. *Transition time for ocean carbon-cycle model intercomparison.* Research GAIM, Vol. 1, no. 2, Univ. New-Hampshire, Durham, NH, USA.

Peng, T.-H, Takahashi, T., Broecker, W. S. and Olafsson, J. 1987. Seasonal variability of carbon dioxide, nutrients and oxygen in the northern North Atlantic surface water: observations and a model. *Tellus* **39B**, 5, 439–458.

Poisson, A., Metzl, N., Brunet, C., Schauer, B., Brès, B., Ruiz-Pino, D. and Louanchi, F. 1993. Variability of sources and sinks of CO_2 and in the Western Indian and Southern Oceans during the year 1991. *J. Geophys. Res.* **98**, C12, 22759–22778.

Poisson, A., Metzl, N., Danet, X, Louanchi, F., Brunet, C., Schauer, B., Brès, B. and Ruiz-Pino, D. 1994. Air–sea CO_2 fluxes in the Southern Ocean between 25° and 85°E. In: *The polar oceans and their rôle in shaping the global environment* (eds. Johannessen, O. M., Muench, R. D. and Overland, J. E.). AGU, Geophysical Monograph 85, 273–284.

Rintoul, S. R., Donguy, J. R. and Roemmich, D. H. 1997. Seasonal evolution of upper ocean thermal structure between Tasmania and Antarctica. *Deep-Sea Res.* **44**, 7, 1185–1202

Robertson, J. and Watson, A. 1995. A summer-time sink for atmospheric carbon dioxide in the Southern Ocean between 88°W and 80°E. *Deep-Sea Res.* **42**, 1081–1091.

Sabine, C. L. and Key, R. M. 1998. Controls on fCO_2 in the South Pacific. *Mar. Chem.* **60**, 95–110.

Sabine, C. L., Key, R. M., Johnson, K. M., Millero, F. J., Poisson, A., Sarmiento, J. L., Wallace, D. W. R. and Winn, C. D. 1999. Anthropogenic CO_2 inventory of the Indian Ocean. *Global. Biogeochem. Cycles*, in press.

Schneider, B. and Morlang, J. 1995. Distribution of the CO_2 partial pressure in the Atlantic ocean between Iceland and the Antarctica peninsula. *Tellus* **47B**, 93–102.

Siegenthaler, U. and Sarmiento, J. L. 1993. Atmospheric carbon dioxide and the ocean. *Nature* **365**, 119–125.

Tans, P. P., Fung, I. Y. and Takahashi, T. 1990. Observational constraints on the global atmospheric CO_2 budget. *Science* **247**, 1431–1438.

Takahashi, T., Olafsson, J., Goddard, J. G., Chipman, D. W. and Sutherland, S. C. 1993. Seasonal variation of CO_2 in the high-latitude surface oceans: a comparative study. *Global Biogeochem. Cycles* **7**, 843–878.

Takahashi, T., Feely, R., Weiss, R. F., Wanninkhof, R. H., Chipman, D. W., Sutherland, S. C. and Takahashi, T. T. 1997. Global air–sea flux of CO_2: an estimate based on measurements of sea–air pCO_2 difference. *Proc. Natl. Acad. Sci. USA* **94**, 8292–8299.

Teal, J. M. and Kanwisher, J. 1966. The use of pCO_2 for the calculation of biological production, with examples from waters off Massachusetts. *J. Marine Res.* **24**, I, 4–14.

Wanninkhof, R. 1992. Relationship between wind speed and gas exchange over the ocean. *J. Geophy. Res.* **97**, C5, 7373–7382.

Wanninkhof, R. and Thoning, K. 1993. Measurement of fugacity of CO_2 in surface waters using continuous and discrete sampling methods. *Marine Chem.* **44**, 189–204.

Waterman, L. S. 1965. Carbon dioxide in surface waters. *Nature* **4976**, 1099–1100.

Weiss, R. F. and Price, B. A. 1980. Nitrous oxide solubility in water and seawater. *Marine Chem.* **8**, 347–359.

Weiss, R. F., Jankhe, R. A. and Keeling, C. D. 1982. Seasonal effects of temperature and salinity on the partial pressure of CO_2 in seawater. *Nature* **300**, 511–513.

Weiss, R. F., Van Woy, F. A. and Salameh, P. K. 1992. *Surface water and atmospheric carbon dioxide and nitrous oxide observations by shipboard automated gas chromatography: results from expeditions between 1977 and 1990*. SIO 92-11. ORNL/CDIAC-59, NDP-044. Carbon Dioxide Information Analysis Center, Oak Ridge National Laboratory, Oak Ridge, Tennessee, USA.

Winn C. D., Mackenzie, F. T., Carrillo, C. J., Sabine, C. L. and Karl, D. M. 1994. Air–sea carbon dioxide exchange in the North Pacific Subtropical Gyre: implications for the global carbon budget. *Global Biogeochem. Cycles* **8**, 157–163.

Winn, C. D., Li, Y.-H., Mackenzie, F. T. and Karl, D. M. 1998. Rising surface ocean dissolved inorganic carbon at the Hawaii Ocean Time-series site. *Marine Chem.* **60**, 1/2, 33–47.

Wong, C. S. and Chan, Y.-H. 1991. Temporal variations in the partial pressure and flux of CO_2 at ocean station P in the subarctic northeast Pacific Ocean. *Tellus* **43B**, 206–223.

Wong, C. S., Chan, Y.-H., Page, J. S., Smith, G. E., Bellegay, R. D. and Iseki, K. 1995. Geographical, seasonal and interannual variations of air–sea CO_2 exchange in the subtropical Pacific surface waters during 1983–88 (I). Variabilities of oceanic fCO_2. *Tellus* **47B**, 4, 414–430.